"Numerical Analysis on Thermal Crack Initiation due to Non-Homogeneous Solder Coating on the Round Strip Interconnection of Photo-voltaic Modules"

Alireza Eslami Mjad[a,*] and Nduka Nnamdi Ekere[a]
[a]School of Engineering, Faculty of Science and Engineering, University of Wolverhampton Shifnal Road, Priorslee, Telford Shropshire TF2 9NN, UK

Abstract

Solar energy is one of the most widely used renewable energy sources, with photo-voltaic (PV) solar cells/panels now utilized as an important energy source. The strip interconnection between solar cells (used for collecting current from solar cells) is a key PV module component; as poor interconnection reliability can lead to PV module failure. Multi-Busbar is a new type of interconnection which incorporates several round copper wires to help increase the energy conversion and transmission efficiency of PV modules and also to reduce the material costs. The non-homogeneity of the solder coating on the wires (resulting from manufacturing process faults), is one of the main factors that is responsible for the poor connections between the wire and the silver pads; which adversely impacts on the interconnection strength and long term reliability. This paper concerns an investigation of the effect of solder coating non-homogeneity on the thermo-mechanical response of round wires used for PV module interconnections. The study evaluates the two main parameters of non-homogeneity (out of centre value and direction), and also investigates the effect of geometrical parameters. The Extended Finite Element Method in ABAQUS software was used to determine the micro-crack initiation temperature and location for a given joint design. The results show that the cracking temperature is most affected by the direction of solder coating non-homogeneity and the downward vertical direction of out of centre positioning of copper in the solder coating leads to the most reduction in cracking temperature (up to 21%).

Keyword: PV Module, Multi-Busbar interconnection, Non-Homogeneity of Solder Coating, Crack Initiation, Reliability.

1. Introduction

Ribbon interconnections are one of the main components of PV Modules which connect the individual crystalline silicon solar cells and transmit and conduct their electrical current to external circuits. The design of the ribbon interconnection therefore has a direct influence on the efficiency of

* Corresponding author. Tel.: +44 (0)1902 321 703; fax: +44 (0)1902 321 459.
E-mail addresses: a.e.majd@wlv.ac.uk (Alireza Eslami Majd), ndyekere@wlv.ac.u (Ndy Ekere)

the PV module (in terms of energy conversion and transmission) and the long term reliability. The configuration of the interconnection influences the Shading on the PV Cells and the partial shading loss (with partial shading, one part of the solar panel generates lower amount of energy as compared to the other non-shaded part) reduces the performance and efficiency of PV Modules (Pareek et al., 2017). Many efforts focussed on developing new joining materials have been reported, such as that on electrically conductive adhesive (ECA) joints or conductive paste (CP)-assisted low-temperature soldering (CALS) as an adhesive layer to connect the strips to the cells (Song, et al., 2019) and although this leads to a cheaper interconnection solution (use of less solder materials), the interconnections do not have the required high shear strength.

The Multi-Busbar (MBB) Connector is one of the innovative concepts for strip interconnection and solar cell tabbing. The aim of the MBB design is to increase the number of busbars and to reduce the busbars' width and finger cross sections (Schneider et al., 2006). In comparison with conventional interconnection method, the use of the MBB technology leads to a reduction in the series resistance losses, due to the increased number of current paths and the associated uniform current distribution (Schindler et al., 2013) and (Walter et al., 2014). For example, by using 15 wires instead of three traditional rectangular busbars, the finger length can be reduced from 25mm to 5mm and the width of the finger can also be reduced from 50 µm to 17 µm (Braun et al., 2013). This reduction in Ag-paste area results in bringing down the cost of PV modules, by reducing the consumption of silver by up to 89%. In addition, the use of rounded edge wires in the MBB design helps to reduce the shadowing loss as most of the incident light can be reflected onto the wafer surface; helping to increase the power output as well as the efficiency of PV (Braun et al., 2012). However, the MBB Connector has one unresolved design/manufacture challenge; the problem associated with the non-homogeneity of solder coating that is produced around the Cu-wire which can result in weaker solder joints and interconnections (Walter et al., 2014). Figure 1, shows the cross-sectional views of round copper wires with homogeneous and non-homogeneous solder coating.

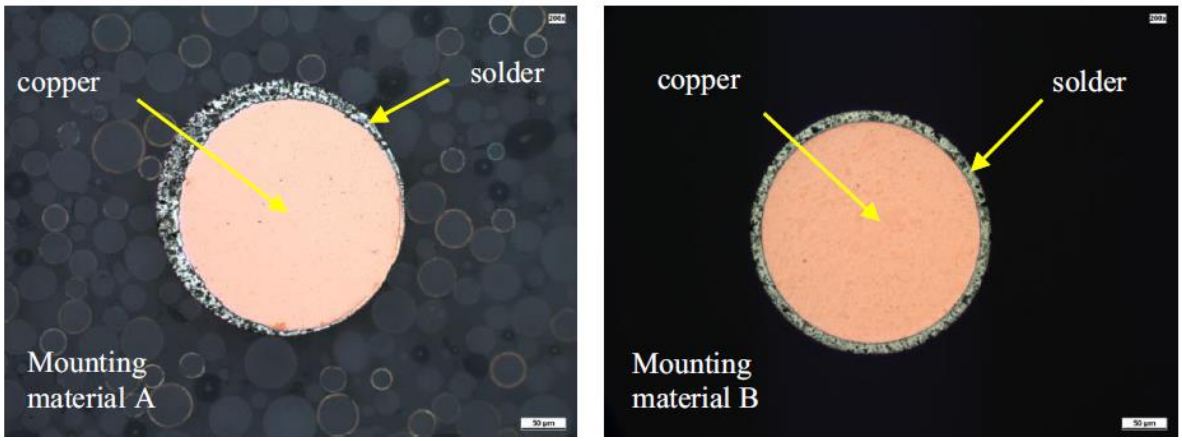

Figure 1 Round wire with non-homogeneous (left) and homogeneous (right) solder coating (Walter et al., 2014)

Thermal stress due to coefficient of thermal expansion (CTE) mismatch between interconnection materials and PV module materials can lead to early interconnection failure and adversely impact on the reliability of the PV module interconnection (O. Ogbomo et al., 2018) and (Zarmai et al., 2016). Indeed, in high temperatures, the weaker MBB solder joint connection area subjected to the thermal stress can develop micro cracks. Previous studies show that the cracks are developed mainly in the contact surface of the strip interconnection and the contact condition can adversely affect the performance of the whole module in terms of power output (Jeong, et al., 2012) and (Itoh et al., 2014). Indeed, the crack developed induces contact resistivity between the Cu ribbon interconnection and cell; resulting in cell-to-module (CTM) loss, hot spot and eventually the disconnection of the bus bar line which consequently results in DC arc (Itoh et al., 2014) and (Tae-hee Jung, 2014).

Rendler et al. have investigated the deformation of cell and thermomechanical stress in both cell and interconnecting wire of MBB PV modules. They found by using lower diameter of wires and by reducing the Young's modulus or the yield strength of the copper, the thermomechanical stress in a solar cell is decreased. They also recognized that the maximum stress in the wires occurs at the edge of the outermost contact pads on both sides of the solar cell (Rendler et al., 2016, 2018). This important region of the solder joint material is where the Intermetallic compound (IMC) is formed. Intermetallic compounds (alloys) form whenever two different metals are soldered together and grow as solid phases during the solidifying of solders on the interface between the solder alloy and its bonding pads (Pecht, 1993). Generally, the thermal fracture of a solder connection due to crack propagation is divided into two distinct modes. Firstly, inside a solder joint (solder-controlled fracture) due to the growing grain size of solder and decreasing bonding strength during thermal cycles, a crack progresses at the interface of large grain. Secondly, at the interface of the solder with interconnection material layers by generating Intermetallic Compounds (IMC) layer such as Cu5Sn6 and Ag3Sn due to the dissolution of Ag/Cu in the solder and the formation of a brittle layer (Itoh et al., 2014). Experimental observations show that the fractures and straight crack path are located on the component side of the solder interconnections (beneath die edge) (Li et al., 2012). Consequently, it is obvious that the IMCs layers in the solder region boundaries play a significant role in the nature of failure and subsequently life time and reliability of solder interconnection. The focus of this study is on the effect of non-homogenous coatings on the strength of brittle micro-cracking in the Intermetallic Compound (IMC) of solder joint in PV module's interconnection.

2. Methodology and Simulation

In this study, we investigate the effect of out of centre of solder coat around copper wire on the crack initiation temperature. Extended Finite Element Method (XFEM) in ABAQUS 6.17 has been utilized to analyse the hot temperature crack initiation (ABAQUS Theory Manual, 2017). XFEM is based on the partition of unity method, and this numerical technique extends conventional finite

element method and allows local enrichment discontinuous functions to be combined with the conventional finite element approximation (Sivakumar & Maji, 2016). One of the main advantages of this method is avoiding any need for re-meshing or geometric crack modelling in numerical simulation, while generating discontinuous fields along a crack and around its tip (Mohammadi, 2008). Unlike conventional FE methods, with the XFEM method there is no need for specifying the location of the crack beforehand. This means that XFEM models a crack within an element as an enriched feature by adding degrees of freedom in elements with special displacement functions (ABAQUS Theory Manual, 2017).

In this study, 2D symmetrical simulation of interconnection strips with four-node plane strain elements (CPE4) is performed as this requires less Computational processing and storage compared to 3D simulation modelling. Altogether, 82 interconnection strip models were simulated in ABAQUS CAE.

Based on Multi-Busbar Connector Prototype specifications published by (Walter et al., 2014), the diameter of copper ribbon and width of silver pad are assumed to be 270 µm and 450 µm, respectively; and the thickness of silver pad and silicon cell are 20 µm and 220 µm (Note: in order to achieve stable response, the gaps between the interconnection strips were considered to be 6mm). To investigate effect of geometrical parameters, four different solder coating thickness (15 µm, 20 µm, 25 µm and 30 µm) were evaluated. In addition, the effect of IMC layer thickness (silver pad interface) was investigated; with four different IMC layer thickness considered (1 µm, 2 µm, 3 µm and 4 µm was used to reflect wide range of soldering temperature). However, the IMC layer thickness on the copper wire core interface is assumed to be 2 µm and symmetry boundary conditions are applied for the bottom of silicon cell. The top edge of Ethylene Vinyl Acetate (EVA) which in contact with the glass protective sheet in PV Module is considered closed in X and Y direction (i.e. no X and Y direction movement is assumed). The temperature of whole solar cell has been increased linearly and isothermally to the crack initiation temperature. Figure 2, shows the discretization and meshing method used in the study and the configuration for the Copper core, Solder Joint, Intermetallic Compound (IMC), Silver Pad, EVA and Silicon cell. A very fine mesh size of 1 µm was used for investigating the effect of the IMC layer thickness on the silver pad interface; and to determine the crack initiation temperature and location of micro-crack.

To meet the requirements of the theory of Linear Elastic Fracture Mechanics (LEFM) which is basis of XFEM for investigation of crack propagation, the IMC layer between solder and silver pad is assumed as a brittle elastic material; whilst all other metallic materials in the PV Module (silver, copper and solder) are considered to have plastic behaviour. Based on the models for traction-

separation laws, different of types of strain and stress components (MAXPS / MAXPE[2], MAXS / MAXE [3] and QUADS/ QUADE[4]) can be used to control damage initiation. In this study, the maximum nominal stress (MAXS) of Shear and Tensile components is considered as the controlling parameters for the damage initiation. This means that the damage (crack) is initiated when these components exceed the defined limits. Then, the initiated crack will be evaluated as Fracture Energy formulations which can be formed by the parameter of Fracture Toughness and Elastic Modulus (Du, 2009).

Table 1 shows the mechanical properties of materials used in the simulation. The temperature dependency of the thermal coefficient of expansion was considered for the Silver, Solder, IMC and copper materials; and the temperature dependency of the Young's Modulus and plastic behaviour was also considered for Solder as shown in Table 2.

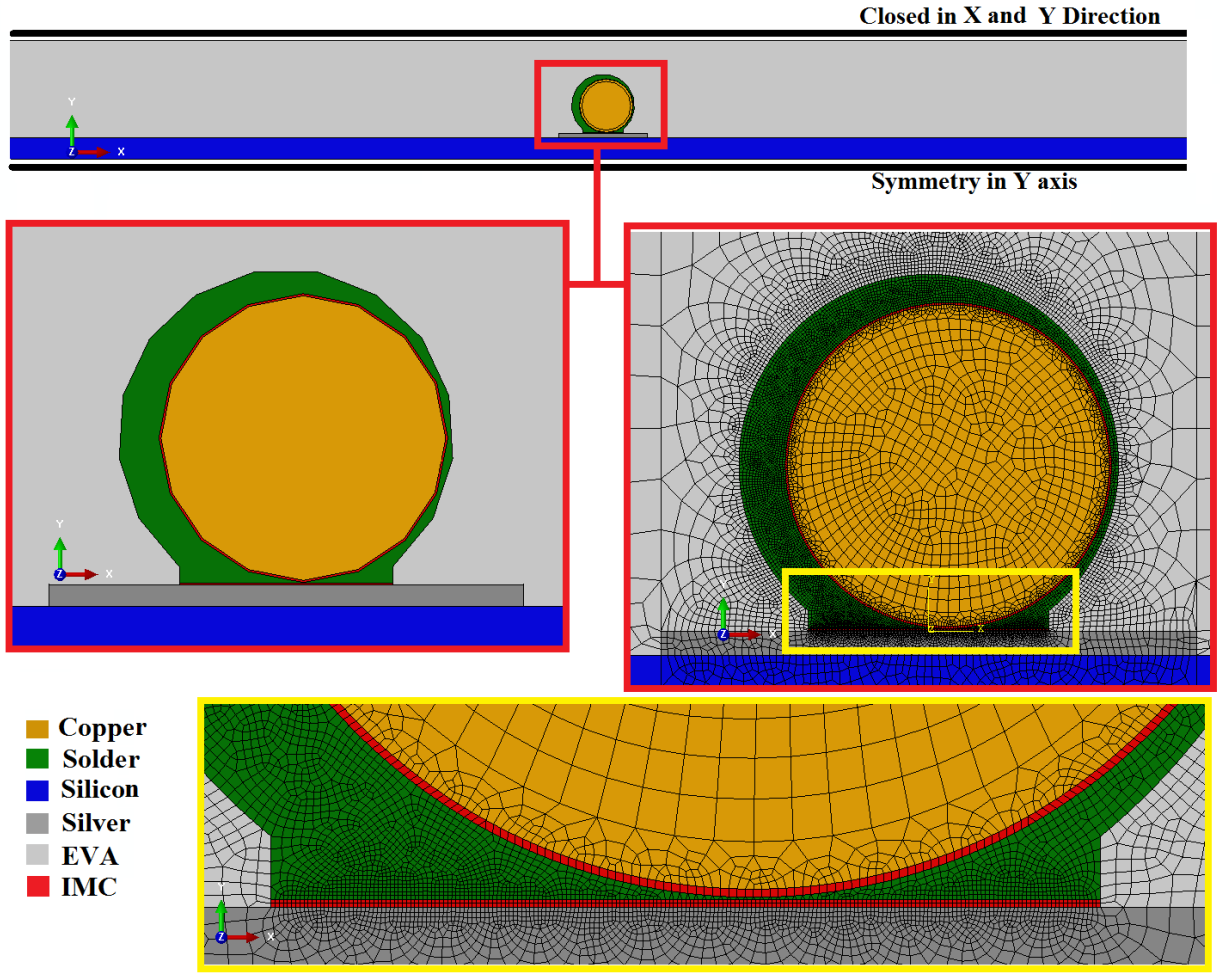

Figure 2 Applied mesh and material arrangement of the PV module Cell in the top interconnecting area

[2] Maximum principal stress (MAXPS) and maximum principal strain (MAXPE)
[3] Maximum nominal stress (MAXS) and maximum nominal strain (MAXE)
[4] Quadratic nominal stress (QUADS) and quadratic nominal strain (QUADE)

Table 1 Mechanical Properties of Material used in the FEM simulation of strip interconnection

Parameter (unit)	**Material**					
	IMC (SnAg)	**Solder Joint**	**Silver** (AZoM, 2001)	**Copper** (Jing, et al., 2015)	**EVA** (Department, 2003)	**Silicon** (Owen-Bellini et al., 2015)
Elastic Modules (MPa)	See Table 2	See Table 2	69	121	11	170
Poisson's Ratio (-)	0.35	0.35	0.365	0.34	0.499	0.28
Yield Stress (MPa)	-	-	43	121	12	170
Shear Strength (MPa) (Deng et al., 2005)	$27.6-1.95*H_{IMC}$	30	-	-	-	-
Tensile Strength (MPa) (Zhong et al., 2010)	65	78	-	-	-	-
Fracture Toughness (MPa.m^0.5)	7	7	40	30	-	0.83
Thermal Expansion Coefficient (ppm/k)	See Table 2	See Table 2	See Table 2	See Table 2	270	2.6
Plastic Stress-Strain Curve (MPa)	-	See Table 2	43@0.001 120@0.04	121@0.001 186@0.004 217@0.01 234@0.02 248@0.04	-	-

Table 2 Temperature dependent properties of interconnection materials

Temp. (c)	**CTE for Copper (ppm/k)** (Taulaukian et al., 1975) (Interpolated)	**CTE for Silver (ppm/k)** (Taulaukian et al., 1975) (Interpolated)	**CTE for Solder (ppm/k)** (49-0.07T) (Li, el al., 2012)	**Solder Young's Modulus (MPa)** (21.3+0.017T) (Li et al., 2012)	**Stress (MPa)** (at 0.0, 0.065 Plastic Strain) (Siviour et al., 2005) (Interpolated)
0	16.22	18.67	21.3	49	71, 145
30	16.60	18.98	21.81	46.9	52, 131
60	16.91	19.20	22.32	44.8	16, 110
90	17.22	19.42	22.83	42.7	-
120	17.53	19.65	23.34	40.6	-
150	17.76	19.91	23.85	38.5	-

The schematic view of cross section of the round ribbon interconnector presented in Figure 3, shows that $\mathbf{S_e}$ (the molten solder area) located between the lower end of strip interconnection and the silver pad is displaced sideways to the both left and right corners of interconnect strip; thereby increasing the contact area between the strip interconnection and silver pad. The mathematical expressions used for calculating the extra contact length $\mathbf{X_m}$ between the solder joint and the Silver pad is given by equation eq. #5. If we assume that the Solder Area $\mathbf{S_e}$ with height $\mathbf{H_e}$ is sub-divided into triangular areas $\mathbf{S_m}$; then the derivation of the extra contact length $\mathbf{X_m}$ is as detailed in eq. #1 - #5.

To investigate the effect of solder joint height on the strength of the strip interconnection, four different molten solder heights $\mathbf{H_e}$ was considered (i.e. $\mathbf{H_e}$ was varied from 25%, 37.5%, 50% to 62.5% of solder coating thickness).

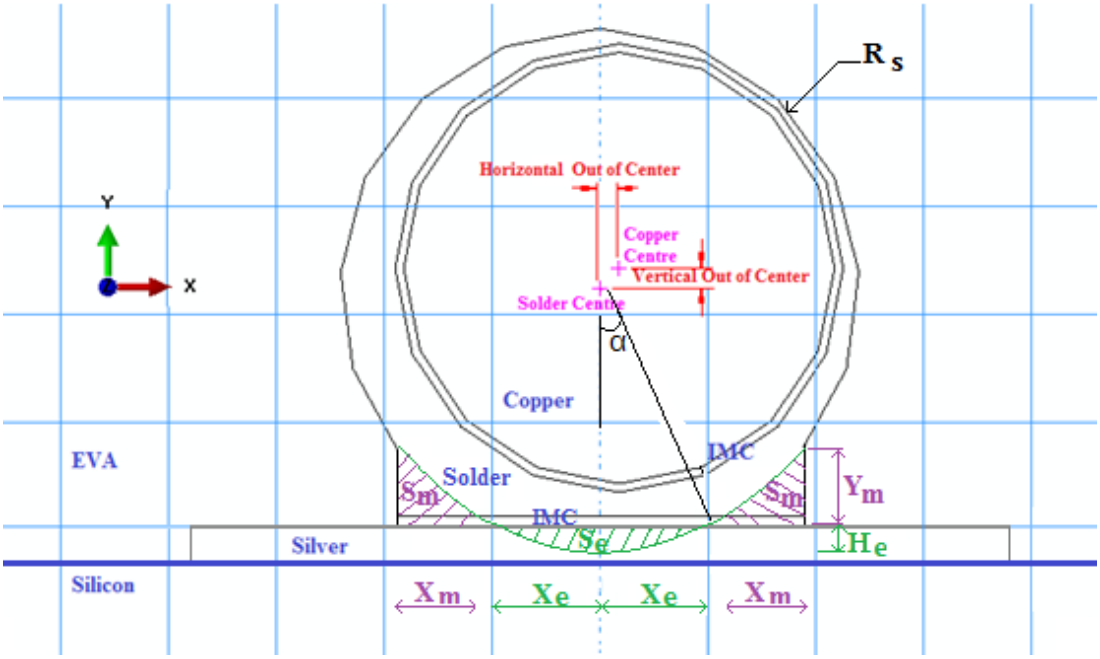

Figure 3 Cross section of round ribbon interconnector with view of vertical and horizontal out of centre

$$\boldsymbol{Eq.1}: \quad X_e = \sqrt{{R_s}^2 - (R_s - H_e)^2}$$

$$\boldsymbol{Eq.2}: \quad tan(\alpha) = \frac{X_e}{R_s - H_e} = \frac{Y_m}{X_m}$$

$$\boldsymbol{Eq.3}: \quad S_e = {R_s}^2.\alpha - 2.X_e.(R_s - H_e)$$

$$\boldsymbol{Eq.4}: \quad S_m = \frac{Y_m.X_m}{2} = \frac{S_e}{2}$$

$$\boldsymbol{Eq.5}: \quad X_m = \sqrt{\frac{S_e}{\tan(\alpha)}} = \sqrt{\frac{{R_s}^2.Arctan\left(\frac{\sqrt{{R_s}^2 - (R_s - H_e)^2}}{R_s - H_e}\right) - \sqrt{{R_s}^2 - (R_s - H_e)^2}.(R_s - H_e)}{\frac{\sqrt{{R_s}^2 - (R_s - H_e)^2}}{R_s - H_e}}}$$

3. Results and Discussions

This section presents the results from the study on the investigation of the effect of solder coating non-homogeneity on the thermomechanical response of round copper wires used for PV module interconnections and the evaluation of the effect of three geometrical parameters, namely the Intermetallic Compound (IMC) layer thickness, solder joint height and thickness on the strength of the interconnections.

3.1. Crack location

The results of the XFEM analysis presented in Figure 4 shows the one-micrometre crack that is initiated in the IMC layer between the solder joint material and silver pads. For all the geometrical parameters considered in the study, the results show that the highest stress accumulation (and the micro-crack initiation), occurs at the edge of the IMC layer interface between the solder joint and silver pad. . The results also show that the crack propagation is in the parallel direction to the silver pad. The material properties presented in Table 2, show that the micro-crack at the interface between the solder joint and silver pad is caused by the high coefficient of thermal expansion (CTE) mismatch between solder joint and silicon layer.

Figure 5 shows the Von Mises stress and shear stress contours in the IMC layer between solder coat and Silver pad at the micro-crack initiation temperature and the crack propagation. Although the concentration of shear stress in the IMC layer leads to the micro-crack initiation and propagation along the IMC interface layer; further crack progression can be caused by thermal recycling in hot temperature operation which can lead to the disconnection of the strip interconnection from the Silver pad.

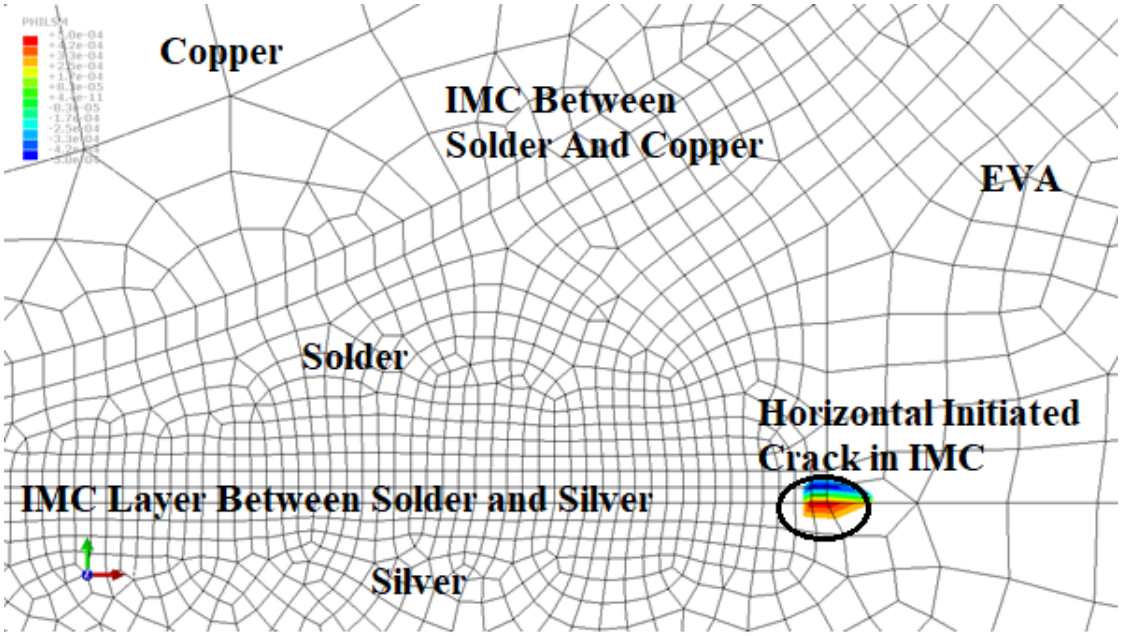

Figure 4 crack initiation in IMC layer between solder coat and Silver pads

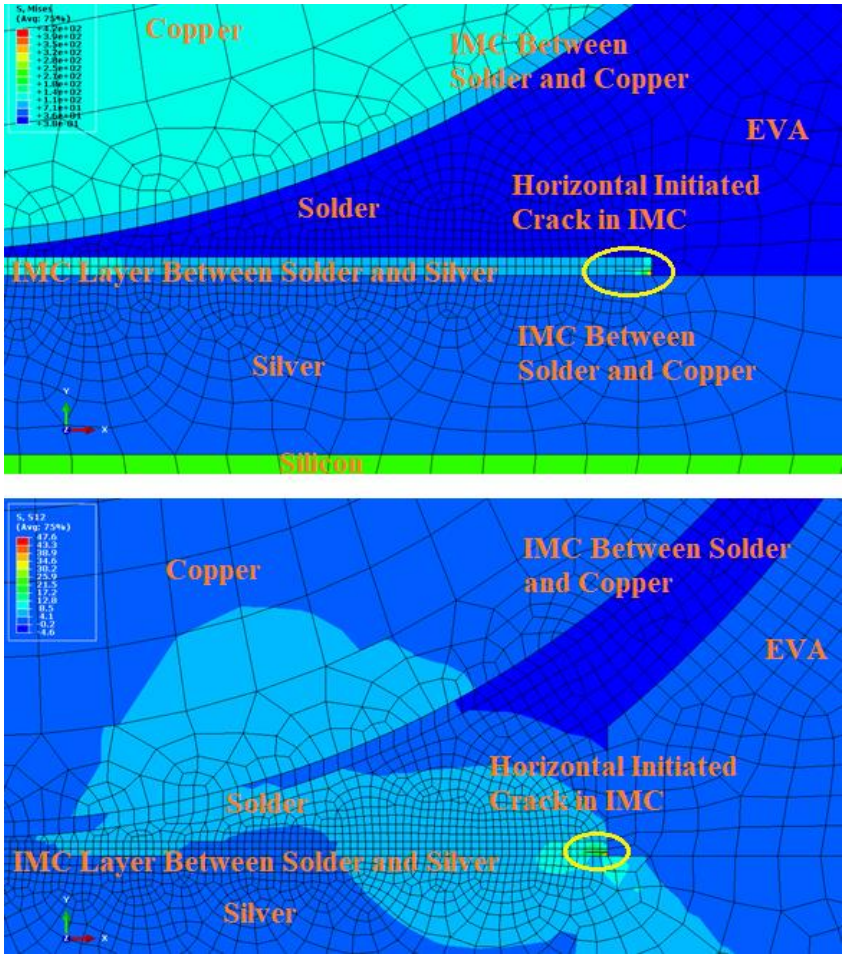

Figure 5 Von Mises Stress (Top) and Shear Stress (Below) Contours in temperatures of micro-cracking of IMC layer between solder coat and Silver pads

3.2. Out of centre positioning of copper in the interconnection strip

Figure 6 shows the crack initiation temperatures for different geometries and out of centre distances in different directions including the upward Y direction (+90 Degrees), the downward Y direction (-90 Degrees), the horizontal (0 Degree) and also the upward and the downward radial directions (-9.5 and +/- 18.5 Degrees). The molten solder height in this graph is considered 50% of solder thickness (10 µm) and the thickness of IMC layer is assumed to be 2 µm. The results of the simulations show that by increasing the out of centre distance (i.e. with more non-homogenous solder coating) in downward directions, the crack initiation strength of the solder joint decreases (Note: the highest rate is for -90 Degree out of centre positioning). This means that for the downward out of centre positioning of the copper inside the coated wire, the crack initiation temperature decreases with increasing non-homogeneity of coating. This is because the narrow solder thickness between copper wire and silicon layer results in an increase in the accumulated strain and thermal stress due to the high thermal coefficient of expansion (CTE) mismatch between the solder and silver materials.. For this reason, the micro-cracks are more likely to occur at the interface between the IMC layer and the silver pad. The results also show that for the upward out of centre positioning of the copper inside the coated wire, the cracking initiation strength of the solder joint is increases with more non-

homogenous solder coating (increases the micro-crack initiation strength); and the crack initiation temperature is also much higher than those for downward out of centre positioning directions.

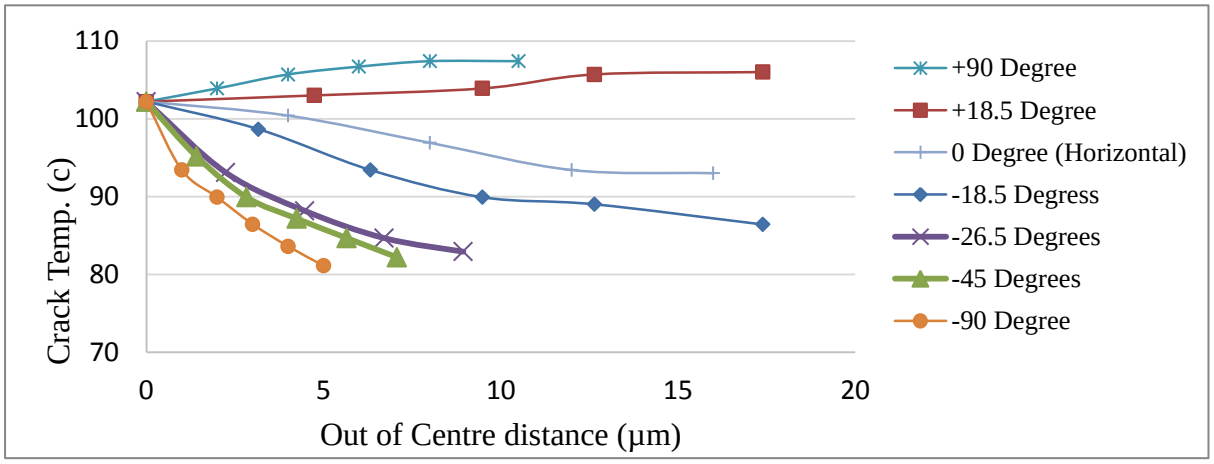

Figure 6 Temperature of crack initiation for different direction of out of centre distances. The molten solder height is 50% of Solder thickness and the thickness of IMC layer is assumed to be 2 µm.

3.3. Molten Solder Height

Figure 7 shows the effect of the out of centre distance in the downward Y direction (-90 Degrees) for different molten solder heights on the crack initiation temperature. In principle, increasing the molten solder height increases the solder contact between the copper wire and the silver pad and hence lead to more reliable connection; the results in Figure 7 suggests that by increasing the molten solder height and increasing solder contact will actually result in micro-cracks occurring at much lower temperatures. This reduction in the micro-crack initiation temperature can be attributed to the high levels of thermal stress resulting from the coefficient of thermal expansion (CTE) mismatch in the increased solder contact. However, the reduction in the micro-crack initiation temperature due out of centring is mitigated by the increase in solder joint strength; and thereby reducing the impact of out of centring with high molten solder height.

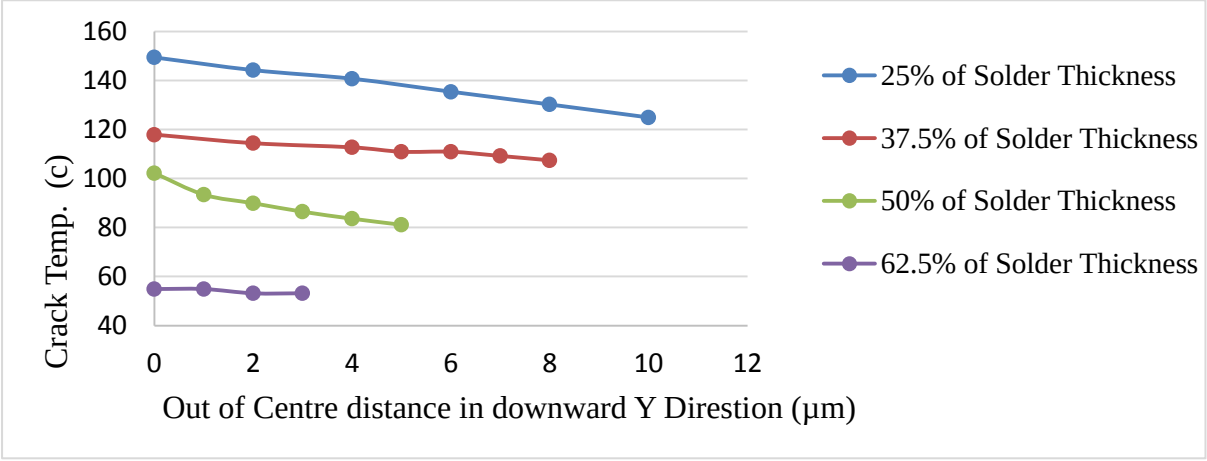

Figure 7 Temperature of crack initiation via out of centre distances in downward Y direction for different molten solder height. Thickness of IMC layer is considered 2 µm.

3.4. Thickness of IMC Interface Layer between strip interconnection and silver pad

Figure 8 demonstrates the effect of out of centre distances in downward Y direction (-90 Degrees) on crack initiation temperature for cases where the solder thickness is 20 µm and the molten solder height is 10 µm (i.e. 50% of solder thickness), with different IMC layer thickness between strip interconnection and silver pad. The results show that solder joints with lower IMC layer thickness exhibited higher strengths than solder joints with higher IMC thickness. The results also show that there is a reduction in the crack initiation temperature with increases in the out of centre positioning; however this is negligible with higher IMC layer thickness.

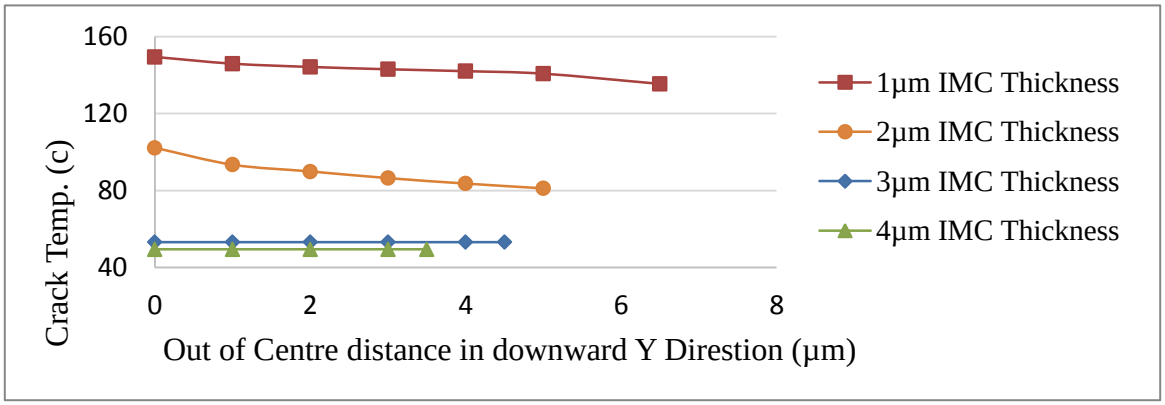

Figure 8 Temperature of crack initiation via out of centre distances in downward Y direction for different IMC layer thickness. The molten solder height is 50% of Solder thickness.

3.5. Solder Coating Thickness

Figure 9 shows the effect of out of centre distances on crack initiation temperature in downward Y direction (-90 Degrees) for cases with 10 µm molten solder height (50% of Solder thickness), IMC layer thickness of 2 µm with different solder thickness. The result shows that for higher solder thickness, increasing the solder thickness reduces the crack initiation temperature; but the effect of out of centre distance on crack initiation temperature is negligible.

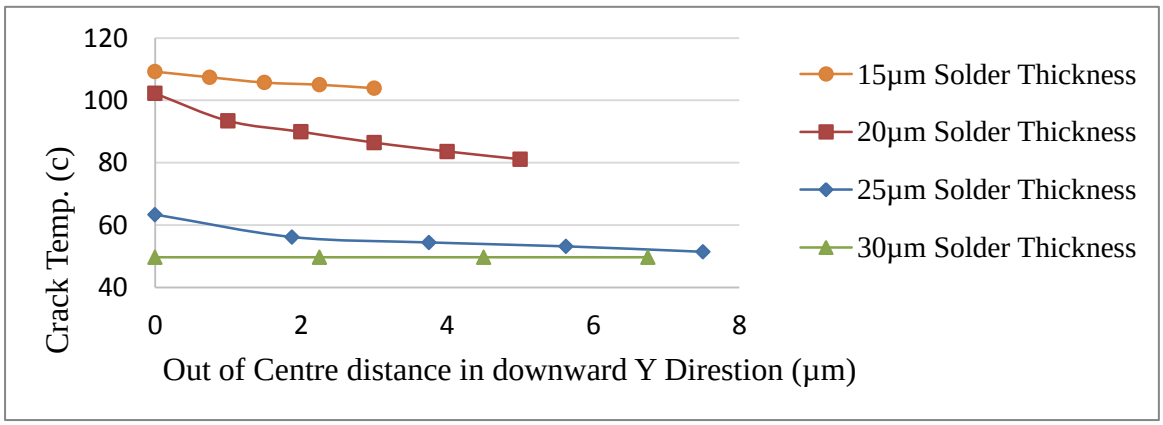

Figure 9 Temperature of crack initiation via out of centre distances in downward Y direction for different solder thickness. The molten solder height is 10 µm and the IMC layer thickness is 2 µm.

4. Conclusion

This study presents the results of the Extended Finite Element Method (XFEM) Simulation performed on the round wire used in Multi-Busbar (MBB) strip interconnection of solar PV module to evaluate micro-crack initiation in non-homogenous solder coating at high temperatures. The determination of the conditions for micro-crack initiation in the solder coating on the round wire is important for determining the interconnection design parameters that will ensure long term reliability of the solar PV module. The results from the simulation study would be used for MBB interconnection design and for the evaluation of solar PV module performance and reliability. The study evaluates the two main parameters of non-homogeneity (out of centre value and direction), and also investigates the effect of geometrical parameters including Intermetallic Compound (IMC) layer thickness and solder joint height. The XFEM in ABAQUS 6.17 software package was used to determine the hot temperature required for micro-crack initiation for each joint design. Also, XFEM analysis was used to predict the location of the micro- crack in the IMC layer between solder coating and silver pad.

The results show that the micro-crack is initiated in the parallel direction with silver pad and the initiation temperature is most affected by the direction of solder coating non-homogeneity and the downward vertical direction of out of centre positioning of copper in the solder coating leads to the most reduction in crack initiation temperature (up to 21% reduction was observed for the case 5.5 µm out of centre distance). The results also show that by increasing the amount of molten solder/solder thickness, the micro-crack initiation will take place at a lower temperature due to high thermal stress accumulation in the IMC layer. Also, it was found that at high solder thickness the micro-crack initiation temperature is less affected by non-homogeneity. The results also show that increasing the IMC layer thickness leads to a decrease in the micro-crack initiation temperature threshold and thinner IMC layers are more sensitive with non-homogeneity. The results of the study will also be useful for researchers in evaluating the impact of IMCs layers in the solder region boundaries on solar PV module reliability and in developing design-for-reliability guidelines.

References

ABAQUS, I., 2017. *ABAQUS User's and Theory Manuals; Version 6.17,* s.l.: ABAQUS, Inc.: Providence Rhode Island, RI, USA.

AZoM, 2001. *Silver - Applications and Properties of Silver.* [Online]
Available at: https://www.azom.com/properties.aspx?ArticleID=600

Braun, S. et al., 2013. *The multi-busbar design: an overview.* s.l., s.n., p. 86 – 92.

Braun, S., Micard, G. & Hahn, G., 2012. *Solar cell improvement by using a multi busbar design as front electrode.* s.l., s.n., pp. 227-233.

Deng, X., Sidhu, R. j. & Chawla, N., 2005. Influence of reflow and thermal aging on the shear strength and fracture behavior of Sn-3.5Ag Solder/Cu joints. *Metallurgical and Materials Transactions A 36(1),* pp. 55-64.

Department, C. U. E., 2003. *Materials Data Book.* Cambridge, UK: Cambridge University Engineering Department Data Books.

Du, Z.-z., 2009. *eXtended Finite Element Method (XFEM) in Abaqus.* [Online] Available at: http://www.simulia.com/download/rum11/UK/Advanced-XFEM-Analysis.pdf

Itoh, U. et al., 2014. *Solder joint failure modes in the conventional crystalline Si module.* s.l., s.n.

Jeong, J.-S., Park, N. & Han, C., 2012. Field failure mechanism study of solder interconnection for crystalline silicon photovoltaic module. *Microelectronics Reliability.*

Jing, X. et al., 2015. *Effect of pre-CMP annealing on TSV pumping in thermal budget and reliability test.* Hsinchu, Taiwan, IEEE 22nd International Symposium on the Physical and Failure Analysis of Integrated Circuits.

Karppinen, J., Laurila, T., Ka, J. & Li, J., 2012. Reliability of Lead-Free Solder Interconnections in Thermal and Power Cycling Tests. *IEEE TRANSACTIONS ON COMPONENTS AND PACKAGING TECHNOLOGIES, VOL. 32, NO. 2.*

Mohammadi, S., 2008. *Extended Finite Element Method: For Fracture Analysis of Structures.* s.l.:Wiley/Blackwell.

O. Ogbomo, O., H. Amalu, E., Ekere, N. & P.O., O., 2018. Effect of operating temperature on degradation of solder joints in crystallin esilicon photovoltaic modules for improved reliability in hot climates. *Solar Energy 170,* p. 682–693.

Owen-Bellini, M., Zhu, J., R. Betts, T. & Gottschalg, R., 2015. *Thermo-Mechanical Stresses of Silicon Photovoltaic Modules.* Bangor, United Kingdom, s.n.

Pareek, S., Chaturvedi, . N. & Dahiya, R., 2017. Optimal interconnections to address partial shading losses in solar photovoltaic arrays. *Solar Energy 155,* p. 537–551.

Pecht, M., 1993. *Soldering processes and equipment.* s.l.:Wiley-IEEE. p. 18. ISBN 978-0-471-59167-2. .

Rendler, L. C. et al., 2016. *Mechanical stress in solar cells with multi busbar interconnection-Parameter study by FEM simulation.* s.l., s.n.

Rendler, L. C., Walter, J., Goldenberg, S. & Bein, A., 2018. Mechanical and electrical properties of wave-shaped wires for low-stress interconnection of solar cells. *Solar Energy Materials and Solar Cells 176,* p. 204–211.

Schindler, S. et al., 2013. *Soldering process and material characterization of miniaturized contact structures of a newly developed multi busbar cell metallization concept.* s.l., s.n., p. 480–483.

Schneider A, Rubin L & Rubin G, 2006. *Solar Cell Efficiency Improvement by New Metallization Techniques - the Day4 Electrode Concept.* Wikoloa, Hawaii, USA, 4th IEEE World Conference on Photovoltaic Energy Conversion.

Sivakumar, G. & Maji, V., 2016. Simulation of crack propagation in rocks by XFEM. *Recent Advances in Rock Engineering (RARE 2016).*

Siviour, C. R., Walley, S., Proud, W. & Field, J., 2005. Mechanical properties of SnPb and lead-free solders at high rates of strain. *Journal of Physics D: Applied Physics,* p. 4131–4139.

Song, H.-J.et al., 2019. Conductive paste assisted interconnection for environmentally benign leadfree ribbons in c-Si PV modules. *Solar Energy 184,* pp. 273-280.

Tae-hee Jung, H.-e. S. H.-k. A. G.-h. K., 2014. A mathematical model for cell-to-module conversion considering mismatching solar cells and the resistance of the interconnection ribbon. *Solar Energy 103,* p. 253–262.

Taulaukian, Y., Kirby, R., Taylar, R. & Desai, P., 1975. *Thermal expansion Metallic Elements and Alloys-THERMOPHYSICAL PROPERTIES OF MATTER. VOLUME 12.* New York: SPRINGER SCIENCE+BUSINESS MEDIA, LLC.

Walter, J. et al., 2014. *Multi-wire interconnection of busbar-free solar cells.* s.l., s.n., p. 380–388.

Zarmai, M. T., Ekere, N., Oduoza, C. & H. Amalu, E., 2016. Optimization of thermo-mechanical reliability of solder joints in crystalline silicon solar cell assembly. *Microelectronics Reliability,* p. 117–125.

Zhong, W., QIN , F., AN, T. & WANG, T., 2010. *Mechanical Properties of Intermetallic Compounds in Solder Joints.* s.l., s.n.